On the Dynamics of a Vertically Driven Damped Planar Pendulum

M. V. Bartuccelli*, G. Gentile†, K. V. Georgiou*

* *Department of Mathematics and Statistics, University of Surrey, Guildford, GU2 7XH*

† *Dipartimento di Mathematica, Università di Roma Tre, Roma, I–00146, Italy*

Abstract

Results on the dynamics of the planar pendulum with parametric vertical time-periodic forcing are reviewed and extended. Numerical methods are employed to study the various dynamical features of the system about its equilibrium positions. Furthermore the dynamics of the system far from its equilibrium points is systematically investigated by using phase portraits and Poincaré sections. The attractors and the associated basins of attraction are computed. We also calculate the Lyapunov exponents to show that for some parameter values the dynamics of the pendulum shows sensitivity to initial conditions.

Keywords: basins of attraction; attractors; Poincaré sections, Lyapunov exponents

1 Introduction

Over the last decades parametrically excited nonlinear oscillators have begun to be extensively studied, both theoretically and numerically. Their dynamics is generally very complicated even when only one and a half degrees of freedom are involved: this shows that the complex behaviour does not arise from a large number of variables, but from the nonlinearity of the equation of motion.

Below, a planar pendulum whose point of support (pivot) is subjected to vertical sinusoidal displacement is studied. This system has two equilibrium configurations: the downward position and the upward position. It is known that the upward equilibrium state can be made stable by subjecting the pivot to a harmonic vertical oscillation of appropriate frequency and amplitude. Stephenson (1908) was the first who predicted theoretically this remarkable result, and the idea has reappeared in a number of subsequent studies (Ness 1967, Kalmus 1970, Koch *et al.* 1983, 1985, Michaelis 1985; Pippard 1987; Leiber & Risken 1988; Blackburn *et al.* 1992a, 1992b; Acheson 1993, 1995, 1997).

Analytically, in the absense of friction, the stability of the upward position is usually obtained by the method of *averaging* (see Kapitsa 1951, Landau & Lifshitz 1976 or Percival & Richards 1982), which, however, is not completely satisfactory as pointed out in Blackburn *et al.* 1992b and in Bartuccelli *et al.* 2000a; more specifically in Bartuccelli *et al.* 2000a we rigorously show that the upward position can become stable by proving the existence of KAM invariant curves arbitrarily close to the equilibrium point: such curves produce a topological obstruction for the trajectories arising from initial data contained in the open bounded region internal to them. In Bartuccelli *et al.* 2000b we consider the same situation, but in the presence of (small) friction (as in the present paper), and we prove that the upward equilibrium position of the driven pendulum does indeed become stable if the period of the forcing is small enough, in agreement with both numerical computations and graphic visualization.

In this paper we employ numerical techniques to make detailed studies of such a system in the presence of friction. We shall investigate the stability of both fixed points and study their basins of attraction when they are (asymptotically) stable. We shall also investigate the existence of other attractors, and again determine the corresponding basins of attraction; analogous results for similar models can be found in literature (see Smith & Blackburn 1989, 1992, Blackburn *et al.* 1992a, 1992b, Capecchi & Bishop 1994). Furthermore we also find strong numerical evidence that the union of the

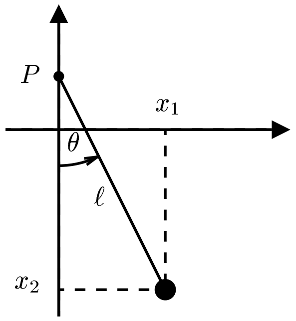

Figure 1: The pendulum with the point of support oscillating on a vertical line.

basins of attraction fills the entire phase space: in other words *any* initial condition will eventually end up to one of the attractors. As far as we know, such a result has not appeared in the literature so far.

Numerical Poincaré sections (see Poincaré 1899, Henon 1982, Hilborn 1994) and phase portraits (see Doerner *et al.* 1994, Heng *et al.* 1994, Baker & Gollub 1996) have been employed to show that, according to appropriate parameters values, the motion of the pendulum can be either regular or chaotic.

In general the results depend strongly upon the values of the parameters: both regular and chaotic attractors can arise, but never simultaneously. A systematic study of all possible scenarios arising by varying the parameters values is certainly interesting, in particular the transition from smooth to chaotic dynamics, but we shall not perform it here, as we are interested rather in showing the complexity of features exhibited by the system: we prefer to concentrate ourselves to some values of the parameters in order to have a general picture.

We compute also the Lyapunov exponents to show sensitivity to initial conditions, thereby corroborating the fact that the system does possess the chaotic dynamics described above for suitable parameters values.

2 A Forced Planar Pendulum

A simple pendulum of mass m and lenght ℓ is constrained to move in a vertical plane under the influence of gravity of intensity g, while its pivot is subjected to a vertical oscillation $y_0(t) = b \cos \omega t$, with positive b and ω; a schematic is shown in Figure 1.

The governing equation of the system is given by:

$$\ddot{\theta} + (\alpha - \beta \cos \tau) \sin \theta = 0, \qquad \tau = \omega t, \qquad \alpha = \frac{g}{\ell \omega^2}, \qquad \beta = \frac{b}{\ell}, \tag{2.1}$$

and the dots denote differentiation with respect to τ. This equation is referred to as the *vertically driven pendulum* equation. Its generalised dimensionless form has the advantages that

1. of the original four parameters (g, ℓ, b, ω) only two (α, β) are left;
2. due to the dimensionless character of all the terms, it can be used to compare directly the dynamics of nonlinear, driven oscillators in any field, for example in mechanics, electrodynamics or solid state physics.

Since the system is 2π periodic in θ, the fixed points are $(0,0)$ and $(\pi,0)$. The $(0,0)$ fixed point corresponds to the downward state of the pendulum, while the $(\pi,0)$ corresponds to the upward state. Equation (2.1) can not be solved anaytically, but if we assume that θ remains near the equilibrium point throughout the motion, it may be linearised: linearization around $(0,0)$ leads to

$$\ddot{\theta} + (\alpha - \beta \cos \tau)\, \theta = 0, \qquad \alpha = \frac{g}{\ell \omega^2}, \qquad \beta = \frac{b}{\ell}, \tag{2.2}$$

while linearization around $(\pi, 0)$, by letting $\xi = \pi + \theta$, leads to

$$\ddot{\xi} + (\alpha + \beta \cos\tau)\,\xi = 0, \qquad \alpha = -\frac{g}{\ell\omega^2}, \qquad \beta = \frac{b}{\ell}, \tag{2.3}$$

where now we naturally take α to be negative (in order to use the same stability diagram for both equations (2.2) and (2.3)); equations (2.2,2.3) are called *Mathieu's equations*. Notice that by changing the sign of β amounts to shifting time by π, and therefore the invariant curves do not depend upon the sign of the parameter β. Figure 2 shows that the solutions of Mathieu's equations, depending on the values of the parameters α and β, are either stable or unstable.

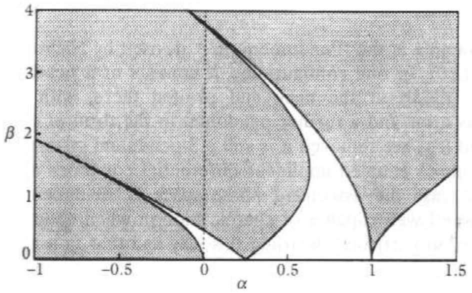

Figure 2: Stability diagram for Mathieu's equations (2.2,2.3). To the right of the dotted line ($\alpha = 0$), the $\theta = 0$ state is unstable in the shaded region, on the left the $\theta = \pi$ state is unstable in the shaded region. Only the region $\beta \geq 0$ is explicitly represented as the diagram is even in β.

Let us consider explicitly some values of the parameters. If $\alpha = 0.5$ and $\beta = 0.1$ the downward state is stable, while if $\alpha = 0.25$ and $\beta = 0.1$ it is unstable; numerically we found that this carries over to the full system (2.1), as shown in Figure 3. Taking equation (2.3), if $\alpha = -0.1$ and $\beta = 0.545$

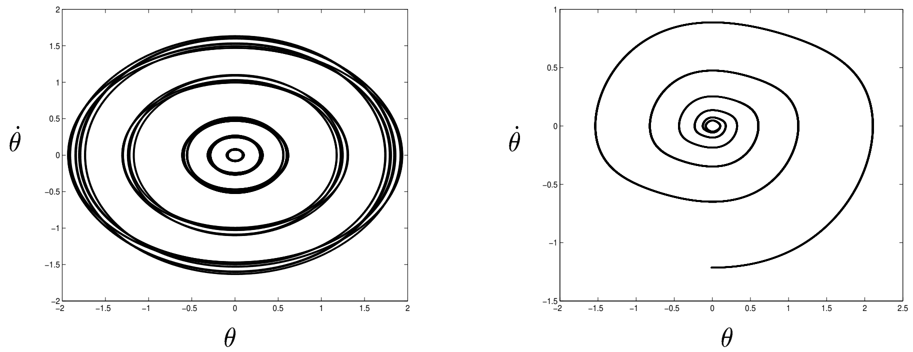

(a) Stable solutions of (2.1) when the linearized system is described by (2.2) with $\alpha = 0.5$ and $\beta = 0.1$.

(b) An unstable solution of (2.1) when the linearized system is described by (2.2) with $\alpha = 0.25$ and $\beta = 0.1$.

Figure 3: Stabilility and instability of the downward state of the pendulum described by (2.1).

we are inside the stability region of the upward state of the pendulum, while if $\alpha = -0.2$ and $\beta = 0.1$ the upward state becomes unstable and the trajectories move away from the fixed point; again we checked numerically that this carries over to the full system, as illustrated in Figure 4.

The presence of friction, unavoidable in any physical context, leads to introduce a damping term into the equation of motion (2.1), which becomes

$$\ddot{\theta} + (\alpha - \beta\cos\tau)\sin\theta + \gamma\dot{\theta} = 0, \tag{2.4}$$

with $\gamma > 0$ denoting the *dissipative coefficient*.

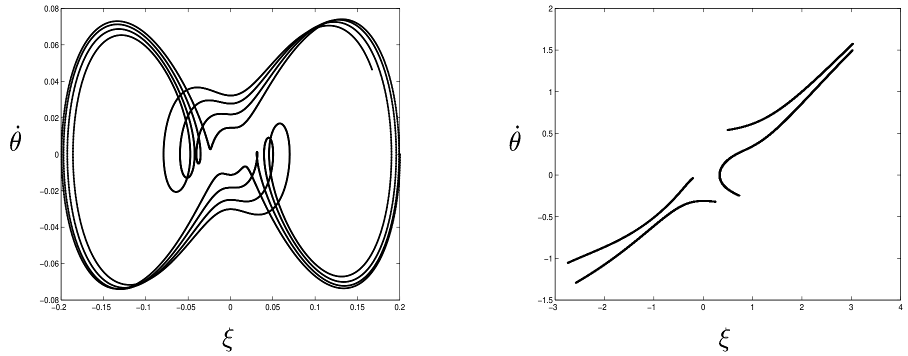

(a) Stable solution of (2.1) when the linearized system is described by (2.3) with using $\alpha = -0.1$ and $\beta = 0.545$.

(b) Unstable solutions of (2.1) when the linearized system is described by (2.3) with $\alpha = -0.2$ and $\beta = 0.1$.

Figure 4: Stabilility and instability of the upward state of the pendulum described by (2.1).

The linearization of (2.4) around the two equilibrium points leads to the same equations (2.2) and (2.3) for the variables $\theta'(t) = e^{\gamma t/2}\theta(t)$ and $\xi'(t) = e^{\gamma t/2}\xi(t)$, respectively, provided that α is replaced with $\alpha' = \alpha - \gamma^2/4$ in both cases; see Jordan & Smith 1977, Ch. 8. Therefore if γ is small enough (for practical purposes one can take γ as done below), for the values of α and β given above the behaviour of the linearized equations in presence of friction (for θ' and ξ') is the same of that of Mathieu's equations (for θ and ξ) obtained for $\gamma = 0$; it is important to note, however, that a stable equilibrium point for the linearized motion of θ' and ξ' becomes asymptotically stable for the linearized motion of the original variables θ and ξ. The stability chart of Mathieu's equation with damping,

$$\ddot{\theta} + (\alpha - \beta\cos\tau)\,\theta + \gamma\dot{\theta} = 0, \tag{2.5}$$

was numerically determined by Leiber & Risken (1988); to compare (2.4) with equation (4) of Leiber & Risken 1988 use that their parameters δ and ε are related to α and β through the relations $\delta = 4\alpha$ and $\varepsilon = 2\beta$.

3 Attractors and Basins of Attraction

Given an attractor, the most direct way of determining a basin of attraction is to numerically integrate the differential equation (2.4) for each possible initial point and record those initial conditions which eventually asymptote to the attractor (see also Blackburn *et al.* 1992b, 1995). This approach has been used to generate high resolution basins containing as many as 1048576 (1024×1024 grid) initial conditions.

To characterise the attractors one can use a *phase portrait* in which the time variable is ignored, by projecting all trajectories either on the plane $(\theta,\dot{\theta})$ when the downward position is stable or on the plane $(\xi,\dot{\theta})$, with $\xi = \pi + \theta$, when the upward position is stable; this can be accomplished by using a DSTOOL package (see Myers *et al.* 1991).

Suppose for argument's sake that we are studying a case in which the downward position is stable, so that we project the trajectory on the plane $(\theta,\dot{\theta})$.

Note that by projecting the motion some information could be lost as to the motion of the full system: for instance a trajectory which when projected gives a closed curve can have in principle any period or could even be quasi-periodic in the space $(\theta,\dot{\theta},\tau)$. We could also use Poincaré sections (as we shall do in next section), by sampling the motion at fixed times: in this way, for instance, a periodic trajectory for the full system (including the time) should appear as a set of points in the plane $(\theta,\dot{\theta})$. Nevertheless we prefer here to project the motion on the plane $(\theta,\dot{\theta})$, as this can be easier if we are only interested to reveal the smooth character of the dynamics.

Once an attractor has been found to determine its basin of attraction we can proceed as follows. First a small target area around the attractor is specified in the plane $(\theta,\dot{\theta})$; for instance if the attractor is the fixed point itself we can take a small rectangle of dimension 0.20×0.20 around the origin, while if the attractor is a closed curve we can take a thin strip of diameter 0.20 around the curve. Points were then selected from the grid of initial conditions and for each one a fourth order Runge-Kutta integration routine was used to numerically integrate the system over an initial transient phase; the integration time step (time unit) was set at 0.1 (about one-sixthieth of the drive period). After this phase, which was typically 4000 time units, a further period of integration was specified and if at any time the solution, when projected into the plane $(\theta, \dot{\theta})$ entered the target area and remained there for several more time units it was assumed that that initial condition belonged to the basin of attraction for that attractor, since other attracting states were far away from the target area.

By using the above method we shall investigate the basins of attraction of our system for various values of the parameters:

- $\alpha = 0.5, \beta = 0.1, \gamma = 0.03$; *these values of the parameters correspond to the stability of the downward state of the linearized dynamics of the pendulum.*

- $\alpha = -0.1, \beta = 0.545, \gamma = 0.08$; *these values of the parameters are in a region of stability for Mathieu's equation, and they correspond for the upside-down pendulum to be stable; the dissipative coefficient is not too small because it is more difficult to stabilize numerically the pendulum in its upward state.*

- $\alpha = 0.02, \beta = 0.35, \gamma = 0.03$; *for this set of values we have stability for both the upward and downward position of the linearized dynamics of the pendulum.*

Note that the dissipative coefficient should not be too small in order to stabilize numerically the equilibium positions; on the other hand it should not be too large either if one wants the stability chart of the linearized system to give some informations about the stability of the full system.

3.1 Attractors and Basins of Attraction for $\alpha = 0.5$, $\beta = 0.1$ and $\gamma = 0.03$

In this subsection we investigate the system (2.4) for the values of the parameters $\alpha = 0.5$, $\beta = 0.1$ and $\gamma = 0.03$. We have found that there are four coexisting attractors: the stationary state $(\theta, \dot{\theta}) = (0, 0)$, an oscillating solution, a clockwise running solution and a counterclockwise running solution (see Figure 5).

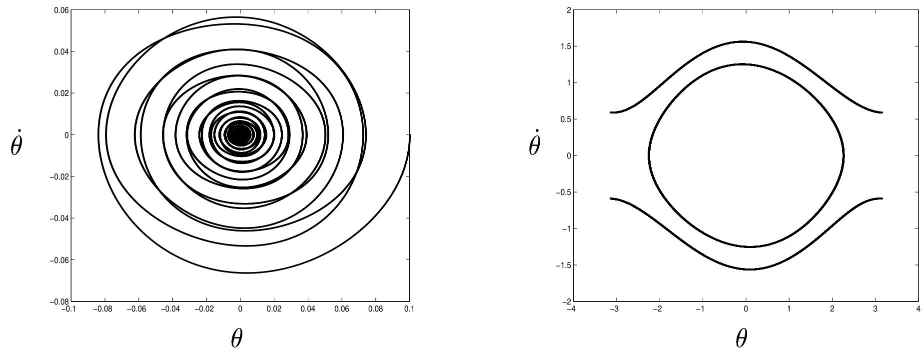

(a) A spiral orbit that goes toward the fixed point attractor.

(b) The oscillating and the two rotating solutions.

Figure 5: Attractors for the vertically driven pendulum with $\alpha = 0.5$, $\beta = 0.1$ and $\gamma = 0.03$.

We show in Figure 6a the basin of attraction for the stationary solution, in Figure 6b the basin of attraction for the oscillating solution, finally in Figure 6c the basins of attraction for the clockwise and anticlockwise running solutions.

For initial conditions inside the black region in Figure 6a, the trajectories converge to the fixed point $(\theta, \dot{\theta}) = (0, 0)$ as shown in Figure 5a. For initial conditions that are inside the black region in Figure 6b, an oscillatory behaviour can be observed after some transients: the trajectories converge to a periodic orbit, whose projection corresponds to the closed curve shown in Figure 5b. Finally

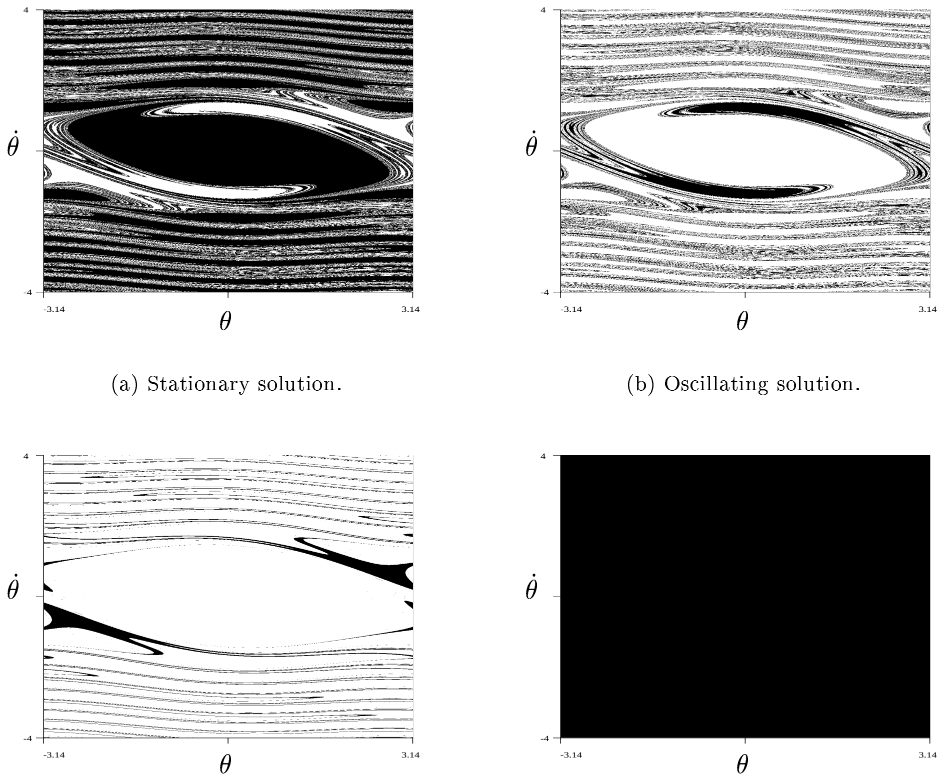

(a) Stationary solution.

(b) Oscillating solution.

(c) Rotating solutions.

(d) Union of all basins.

Figure 6: Coexistence of four basins of attraction (in black) for the vertically driven pendulum with $\alpha = 0.5$, $\beta = 0.1$ and $\gamma = 0.03$.

for initial conditions that are inside the black region in Figure 6c, a clockwise running solution and a counterclockwise running solution can be observed; due to the symmetry of the system, each of these two attractors can be found by rotating the other by π.

Figures 5 show a phenomenon that is characteristic of nonlinear systems but cannot occur in linear systems. For the given system parameters $\alpha = 0.5$, $\beta = 0.1$ and $\gamma = 0.03$, there is a coexistence of four different attractors: depending on the initial conditions, trajectories converge towards one of these attractors (while for linear systems differences in initial conditions are damped out resulting in a single attractor).

There is strong numerical evidence that these four coexisting attractors are the only attractors for the fixed parameters values: any trajectory will ultimately end up to one of the attractors as shown numerically in Figure 6d, where the union of the four basins is represented.

Note that the model is invariant under the symmetry $(\theta, \dot{\theta}, \tau) \to (-\theta, -\dot{\theta}, \tau)$, so that one expects the attractors to be symmetric under inversion with respect to the origin, and in fact this is what happens. On the contrary the model is not invariant under the symmetry $(\theta, \dot{\theta}, \tau) \to (-\theta, \dot{\theta}, -\tau)$: in particular this means that the phase portrait representation of the attractors given in Figure 5b is not symmetric under reflection with respect to the axis $\theta = 0$ (as one can check by looking very carefully at the plots and by computing with accuracy the coordinates of the points of the curves). The apparent symmetry is due to the small value of γ: for $\gamma = 0$, i.e. in absence of friction, the symmetry $(\theta, \dot{\theta}, \tau) \to (-\theta, \dot{\theta}, -\tau)$ is restored and any invariant curve must be even in θ). The same symmetry considerations apply to all following plots.

3.2 Attractors and Basins of Attraction for $\alpha = -0.1$, $\beta = 0.545$ and $\gamma = 0.08$

Consider the system (2.4) with $\alpha = -0.1$, $\beta = 0.545$ and $\gamma = 0.08$. For this case we have found that there are three coexisting attractors: the stationary state $(\theta, \dot{\theta}) = (\pi, 0)$, which corresponds to the upward position of the pendulum, and two other attractors which correspond to rotating (running) solutions; see Figure 7b.

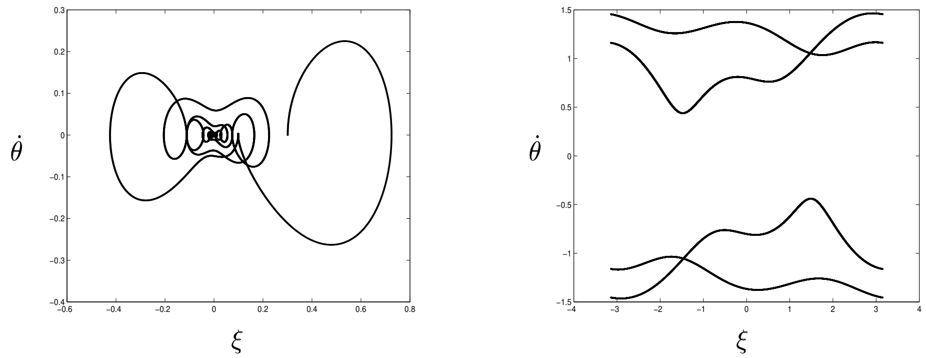

(a) A spiral orbit that goes toward the fixed point attractor.

(b) Rotating clockwise and counterclockwise solutions.

Figure 7: Attractors for the vertically driven pendulum with $\alpha = -0.1$, $\beta = 0.545$ and $\gamma = 0.08$.

We show in Figure 8a the basin of attraction for the stationary solution, and in Figure 8b the basin for the clockwise and anticlockwise running solutions. Note that for each basin there are regions in which the structure seems to be factral (see Smith & Blackburn 1992); for instance Figure 8a reveals a dense core surrounded by fractal layers.

Any initially condition inside the black regions in Figure 8 will ultimately arrive at the corresponding attractor: for initial conditions inside the black region in Figure 8a the trajectories converge to the fixed point attractor $(\theta, \dot{\theta}) = (\pi, 0)$, as shown in Figure 7a, while for initial conditions that are inside the black region in Figure 8b, a clockwise running solution and an anticlockwise running solution can be observed asymptotically as shown in Figure 7b. Also in this case we found that these three attractors are the only attractors (the same picture as in Figure 6d is obtained by drawing simultaneously all the basins represented in Figure 8).

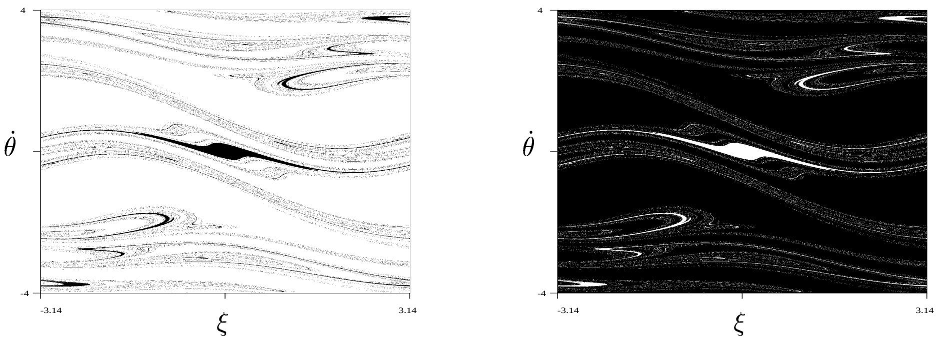

(a) Stationary solution.

(b) Rotating solutions.

Figure 8: Coexistence of three basins of attraction (in black) for the vertically driven pendulum with $\alpha = -0.1$, $\beta = 0.545$ and $\gamma = 0.08$; one has $\xi = \pi + \theta$.

3.3 Attractors and Basins of Attraction for $\alpha = 0.02$, $\beta = 0.35$ and $\gamma = 0.03$

For the parameters values $\alpha = 0.02$, $\beta = 0.35$ and $\gamma = 0.03$ the downward state and the upward state are both stables; in such a case we found that there are five coexisting attractors: the two stationary states $(0, 0)$ and $(\pi, 0)$ (if we use the coordinate θ), an oscillating solution, a clockwise running solution and a counterclockwise running solution; see Figure 9. The corresponding basins of attractions are given in Figure 10; again their union gives the entire phase space.

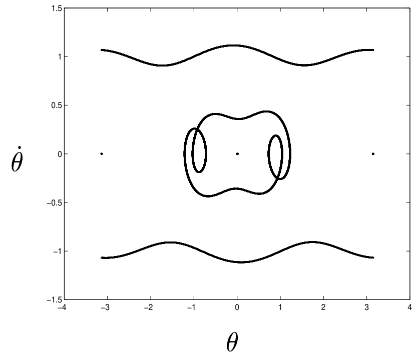

Figure 9: Attractors for the vertically driven pendulum with $\alpha = 0.02$, $\beta = 0.35$ and $\gamma = 0.03$.

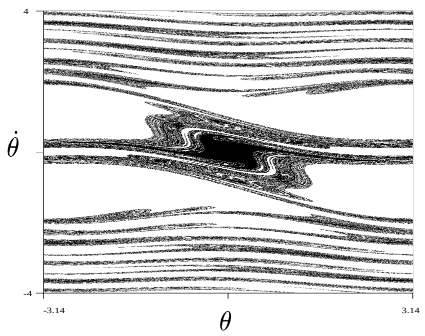

(a) Stationary downward solution.

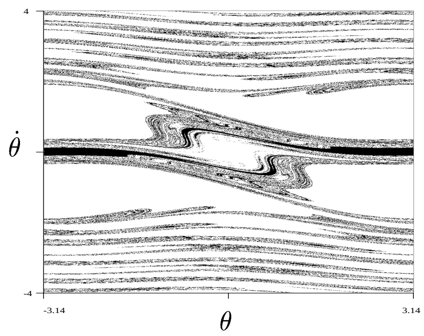

(b) Stationary upward solution.

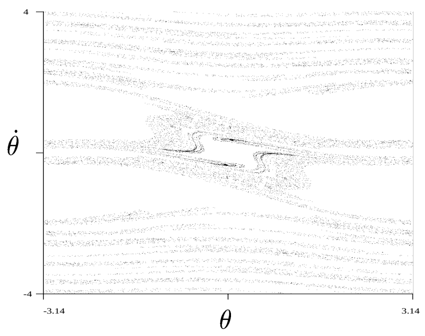

(c) Oscillating solution.

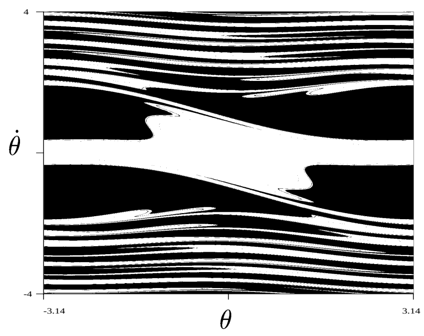

(d) Running solutions.

Figure 10: Coexistence of five basins of attraction (in black) for the vertically driven pendulum with $\alpha = 0.02$, $\beta = 0.35$ and $\gamma = 0.03$.

The values of the parameters α and β considered so far are all inside the stability region in Figure 2 (which describes the linear undamped system). What happens, as a general empirical rule, is that, if an equilibrium position is stable for Mathieu's equations (2.2) or (2.3), then it remains stable *also for the nonlinear damped equation* (2.4); this holds only approximately for the upward position of the pendulum, which would correspond to having a negative value for the parameter α; we refer to Leiber & Risken 1988 for a detailed description of the stability diagram in the linear regime. In the cases considered so far one typically finds coexistence of several smooth attractors, like in the cases explicitly worked out above. The dynamics drastically changes when one takes values of the parameters for which the fixed points attractors are both unstable: in such cases new chaotic attractors may appear, a phenomenon which is well known in literature (see Grebogi *et al.* 1986, Blackburn *et al.* 1992b). We shall discuss it in the next section.

4 Poincaré Sections and Strange Attractors

In this section we analyse the dynamics of our system by fixing α (and γ, so that, for the linearized equation obtained from (2.4) one has a fixed value $\alpha' = \alpha - \gamma^2/4$; see Sect. 2) and by scanning values of β along a vertical line in the plane (α, β).

We have computed the *Poincaré sections* (see Koch *et al.* 1983, 1985, Leven *et al.* 1985, Michaelis 1985) obtained by removing one of the phase space dimensions (in our case the time 'τ'). The key point is that this simplified geometry nevertheless contains the essential information about the possible chaoticity of the system's dynamics. Since our system has a natural period associated with it, i.e. the period of the forcing term, then the plane of the Poincaré sections could be a surface corresponding to a definite but arbitrarily chosen phase of that forcing (so in our case Poincaré sections and stroboscopic phase representations can be identified; see Eckmann & Ruelle 1985). The choise of the plane is not crucial as long as the trajectories cut the surface transversally, that is the trajectories do not run parallel or almost parallel to the surface as they pass through. In our case the Poincaré sections are formed by recording the values of the angle and the corresponding angular velocity whenever the phase of the periodic force reaches some definite value. The pictures below qualitatively do not change if the sampling phase shift is fixed to other values, with respect to the ones explicitly considered in the figures.

4.1 Poincaré Sections and Strange Attractors for $\alpha = 0.5$ and $\gamma = 0.03$

For α we choose here the value $\alpha = 0.5$; from the stability diagram of Mathieu's equation, in Figure 2, one can see that, for the linear case with $\gamma = 0$, see (2.2), the critical value of β for the stability of the downward state is 0.6058. For the full system (2.4) with $\gamma = 0.03$, one finds numerically for the critical value $\beta_c = 0.6063$: above β_c the stationary downward state for the linear system is unstable.

A *period-doubling* transition to chaos occurs when the parameter β is increased, starting at $\beta = 0.55$. We have detected period-doubling bifurcations up to 32–period; more precisely for $\beta < 0.55$ a period one occurs, and at $\beta = 0.55$, $\beta = 0.618$, $\beta = 0.6352$, $\beta = 0.6391$, $\beta = 0.6401$ period doubling bifurcations occur, leading to orbits with period 2, 4, 8, 16, 32, respectively. For instance for $\beta = 0.63$ the Poincaré sections consist of four dots which show that the system is tending toward an orbit on which the motion is periodic with period 4; see Figure 11b.

For β larger than a value $\beta_d = 0.64018$ the motion is fully chaotic. A typical picture is shown in Figure 11d, which gives the evolution of 1600 initial conditions (disregarding the first few iterates), for $\beta = 0.70$: we think that it represents a *strange attractor* (see Eckmann & Ruelle 1985), because the flow has a positive Lyapunov exponent as we show in Sect. 5 below. Analogous pictures have been found numerically also for similar models (see Doerner *et al.* 1994, Leven *et al.* 1985, Smith *et al.* 1989, Blackburn *et al.* 1992a). By proceeding as in Sect. 3, we found numerical evidence that such an attractor is the only attractor in that regime.

Note that, even if the strange attractor disappears below β_d, there are still initial conditions whose first iterates appear as a sequence of dots lying over the *remnant* of the strange attractor existing above β_d before being swept towards some of the attractors, according to the scenario described by Blackburn *et al.* (1992b) in similar systems. This is shown in Figure 12.

4.2 Poincaré Sections and Strange Attractors for $\alpha = -0.1$ and $\gamma = 0.08$

In this subsection we obtain similar results along the scan line β for $\alpha = -0.1$ and $\gamma = 0.08$. For the linear undamped system (2.3) the critical value for stability is $\beta = 0.618$.

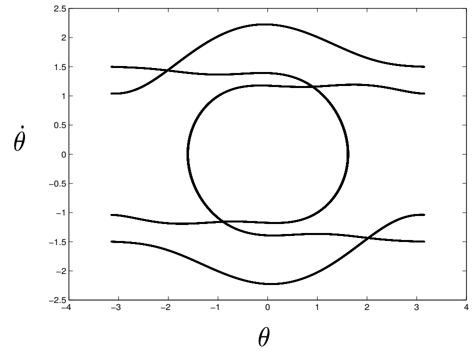

(a) Periodic orbit with period 4 with initial datum $(\theta, \dot{\theta}) = (0.1, 0)$.

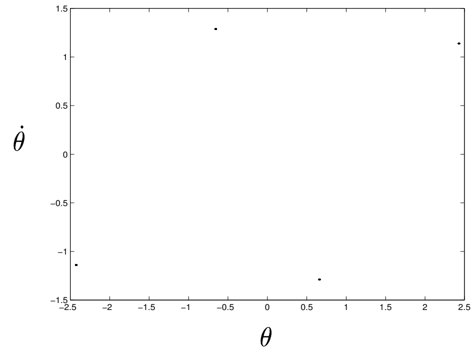

(b) Poincaré section with sampling phase shift of 1 (in radians).

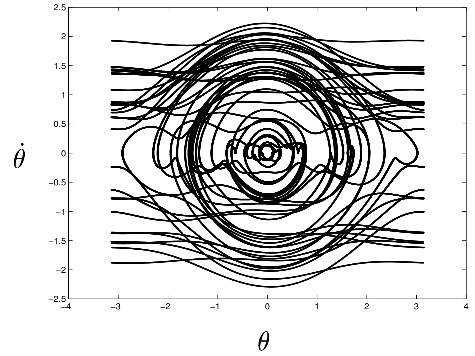

(c) Chaotic trajectory with initial datum $(\theta, \dot{\theta}) = (0.1,0)$.

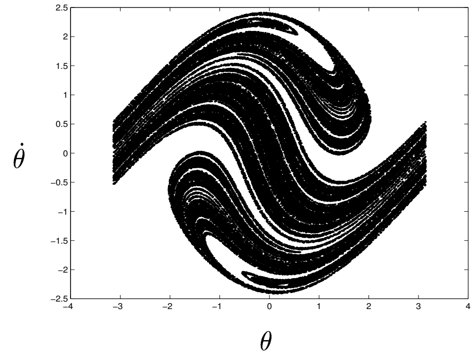

(d) Poincaré section with sampling phase shift of 3 (in radians).

Figure 11: A chaotic trajectory and a periodic trajectory with the corresponding Poincaré sections for $\alpha = 0.5$ and $\gamma = 0.03$. The values of β are respectively $\beta = 0.70$ and $\beta = 0.63$. Transients are disregarded.

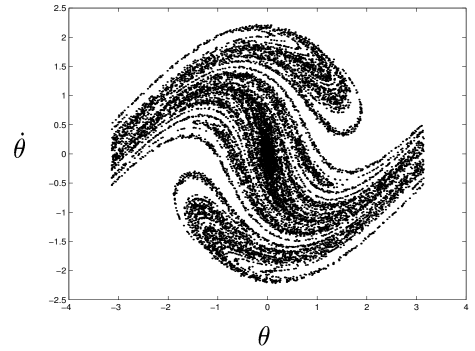

(a) Strange attractor remnant for $\alpha = 0.5$, $\beta = 0.5$ and $\gamma = 0.03$.

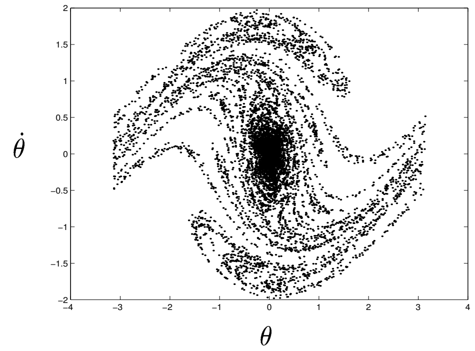

(b) Strange attractor remnant for $\alpha = 0.5$, $\beta = 0.3$ and $\gamma = 0.03$.

Figure 12: Strange attractor remnants for $\alpha = 0.5$ and $\gamma = 0.03$.

For values of β less than $\beta_d = 2.145$ the system have an oscillatory behaviour, and, depending on the value of β, trajectories will eventually end up to a smooth attractor; examples are shown in Figure 13.

The upward state becomes unstable at $\beta_c = 0.623$: then one has a Hopf bifurcation leading to a

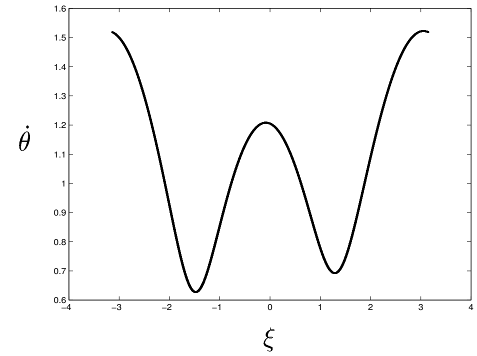

(a) $\alpha = -0.1$, $\beta = 1.2$ and $\gamma = 0.08$.

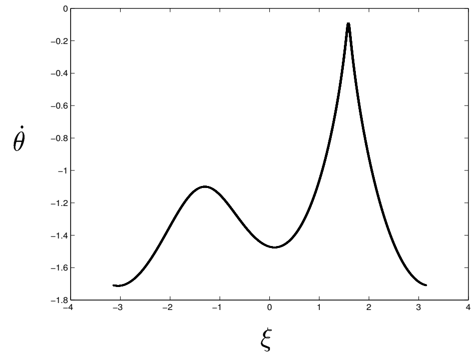

(b) $\alpha = -0.1$, $\beta = 1.5$ and $\gamma = 0.08$.

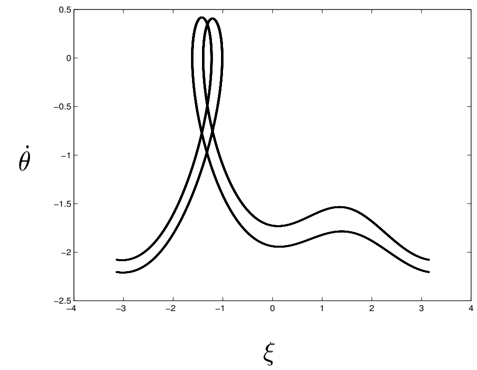

(c) $\alpha = -0.1$, $\beta = 1.8$ and $\gamma = 0.08$;

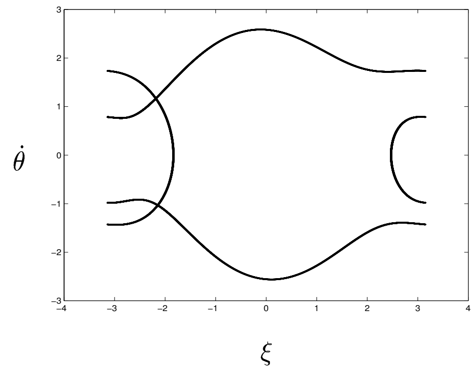

(d) $\alpha = -0.1$, $\beta = 2.1$ and $\gamma = 0.08$.

Figure 13: Smooth attractors (disregarding transients) for $\alpha = -0.1$ and $\gamma = 0.08$.

flutter mode (see Blackburn *et al.* 1992a): for $\beta_c < \beta < \beta_e = 0.679$ the pendulum oscillates around the vertical at half the drive frequency with an amplitude which increases as $\beta - \beta_c$; see Figure 14a. Note that the slight tilt of the projected orbits is consistent with the symmetries of the model

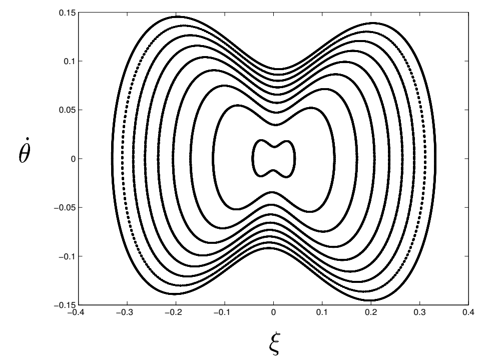

(a)

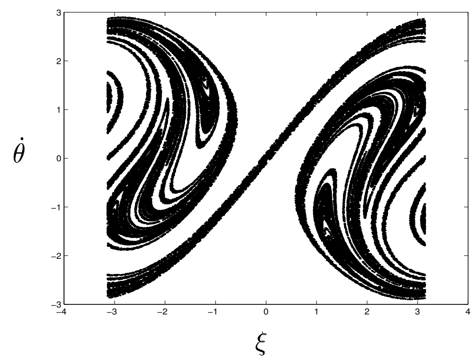

(b)

Figure 14: (a) Oscillating attractors corresponding to the flutter mode for $\alpha = -0.1$ and $\gamma = 0.08$, at different values of $\beta \in (0.623, 0.679)$. (b) Poincaré section for $\alpha = -0.1$, $\beta = 2.2$ and $\gamma = 0.08$, with sampling phase shift of 1 (in radians) of a chaotic trajectory; 1600 orbits as shown (disregarding transients).

(which only require the attractors to be invariant under inversion with respect to the origin); we think that an equivalent tilt should also arise in the comparabale plot in Blackburn *et al.* 1992ba, and that the apparent lack of tilting in Figure 9 of the quoted paper is due to the difficulty to detect it because of the smaller value of γ used there; see the comments at the end of subsection 3.1.

By further increasing β the oscillating orbit disappears and only rotating attractors are left, up to the value β_d: again this is in agreement with the results found by Blackburn *et al.* (1992b) for the same model. For β taking values larger than the value of $\beta_d = 2.145$ the motion is chaotic, as shown in Figure 14b; also this is in accord with the value of 2.20 of the drive amplitude of Blackburn *et al.* 1995.

5 Lyapunov Exponents and Sensitivity to Initial Conditions

We numerically found that, for some parameters values, the Lyapunov exponents are positive, so that there is sensitivity to the initial conditions: this confirms the chaotic character of the motion. For a dissipative system the sum of the exponents must be negative; if the system is chaotic then at least one of the exponents is positive. For our system there are two Lyapunov exponents corresponding to the two dimensions of the phase space $(\theta, \dot{\theta})$. In Sect. 4, we have proposed that the Poincaré section in Figures 11b, 14b represents a strange attractor. We have computed the largest Lyapunov exponent for the same parameters values we chose to obtain Figures 11b and 14b. We found that for $\alpha = 0.5$, $\beta = 0.7$ and $\gamma = 0.03$ the Lyapunov exponent settles down to 0.179563, while for $\alpha = -0.1$, $\beta = 2.2$ and $\gamma = 0.08$ the Lyapunov exponent settles down to 0.207936. For both cases the number of time steps was 10^7 with time unit set at 0.001. In Table 1 we give a list of some computed Lyapunov exponents as β is varied. We should note here that in the chaotic regime the Lyapunov exponent is related with any initial condition that tends to the only existing attractor (i.e. Figures 11b or 14b). In the non chaotic regime, the Lyapunov exponent is related with any initial condition that tends to the corresponding among the rotating attractors found in Sects. 3 and 4.

β	Lyapunov exponents λ
0.63	−0.0140605
0.64	−0.0143172
0.64018	0.0109093
0.64019	0.141205
0.65	0.179953
0.67	0.180256
0.68	0.178863
0.69	0.179888
0.70	0.179563

β	Lyapunov exponents λ
0.8	−0.0399938
0.9	−0.0399802
1.3	−0.039983
1.6	−0.0399905
1.9	−0.0399149
2.14	−0.0395598
2.145	0.0242153
2.2	0.207936
2.5	0.228123

Table 1: Computed Lyapunov exponents as β is varied; the left table corresponds to values of $\alpha = 0.5, \gamma = 0.03$, while the right table correponds to values of $\alpha = -0.1, \gamma = 0.08$.

6 Concluding Remarks

In this paper we investigated a planar pendulum with parametric vertical time-periodic forcing. Numerical techniques were employed to analyse the various dynamical features of the system.

First we studied the stability of the equilibrium states (downward and upward positions) and we verified that, for initial data close to them, there is accordance with the well known theory of Mathieu's equation; furthermore, when such states are stable, we determined numerically their basins of attraction.

Then the existence of other attractors was investigated and their associated basins of attraction were numerically detected. Additionally, we found numerically that these were the only attractors by showing that, depending on the initial conditions, all trajectories converged towards one of them. Such results contribute towards having a more complete picture of the dynamics of this system.

Finally Poincaré sections, phase portraits and sensitivity to initial condiltions provide information about the dynamics of the pendulum for specific values of the parameters α, β and γ. We found that depending on the parameters values the pendulum can show an oscillatory behaviour or an even more complicated time evolution, characterized by the existence of strange attractors. We have strengthened the latter scenario by computing the Lyapunov exponents, which they turn out to be positive as they should.

Acknowledgements

We thank Peter Ashwin and John R Terry for use of their numerical programs for computing the basins of attractions. We also thank Philip J Aston, Philip Kent, Sebastian Reich and John R Terry for their help with the numerics and for useful discussions.

Acknowledgements

D. J. ACHESON, *A pendulum theorem*, Proc. R. Soc. Lond. A **443** (1993), 239–245.

D. J. ACHESON, *Multiple-nodding oscillations of a driven inverted pendulum*, Proc. R. Soc. Lond. A **448** (1995), 89–95.

D. ACHESON, *From calculus to chaos*, Oxford University Press, Oxford, 1997.

D. J. ACHESON & T. MULLIN, *Upside-down pendulums*, Nature **366** (1993), 215–216.

B. L. BAKER & J. P. GOLLUB, *Chaotic dynamics. An introduction*, Cambridge University Press, Cambridge, 1996.

M. V. BARTUCCELLI, G. GENTILE & K. V. GEORGIOU, *KAM theorem and stability of the upside-down pendulum*, Preprint (2000a).

M. V. BARTUCCELLI, G. GENTILE & K. V. GEORGIOU, *On the stability of the upside-down pendulum with damping*, Preprint (2000b).

J. A. BLACKBURN, H. J. T. SMITH & N. GRØNBECH-JENSEN, *Stability and Hopf bifurcations in an inverted pendulum*, Amer. J. Phys. **60** (1992a), 903–908.

J. A. BLACKBURN, H. J. T. SMITH & D. E. EDMUNDSON, *Transient chaos in a parametrically damped pendulum*, Phys. Rev. A **45** (1992b), 593–599.

J. A. BLACKBURN, N. GRØNBECH-JENSEN & H. J. T. SMITH, *Stochastic Noise and Chaotic Transients*, Phys. Rev. Lett. **74** (1995), 908–911.

D. CAPECCHI & S. R. BISHOP, *Periodic oscillations and attracting basins for a parametrically excited pendulum*, Dynam. Stability of Systems **9** (1994), 123–143.

R. DOERNER, B. HÜBINGER, H. HENG & W. MARTIENSSEN, *Approaching nonlinear dynamics by studying the motion of a pendulum. II. Analyzing chaotic motion*, Internat. J. Bifur. Chaos Appl. Sci. Engrg. **4** (1994), 761–771.

J.-P. ECKMANN & D. RUELLE, *Ergodic theory of chaos and strange attractors*, Rev. Mod. Phys. **57** (1985), 617–656.

C. GREBOGI, E. OTT & J. A. YORKE, *Critical exponent of chaotic transients in nonlinear dynamical systems*, Phys. Rev. Lett. **57** (1986), 1284–1287.

E. GRÖLLER, *Application of Visualization tehniques to complex and chaotic dynamical systems*, Preprint (1994).

K. M. HEAL, M. L. HANSEN & K. M. RICKARD, *Maple V learning guide*, Springer, 1996.

H. HENG, R. DOERNER, B. HÜBINGER & W. MARTIENSSEN, *Approaching nonlinear dynamics by studying the motion of a pendulum. I. Observing trajectories in state space*, Internat. J. Bifur. Chaos Appl. Sci. Engrg. **4** (1994), 751–760.

M. HENON, *On the numerical computation of Poincaré Maps*, Phys. D **5** (1982), 412–414.

C. W. HILBORN, *Chaos and nonlinear dynamics*, Oxford University Press, Oxford, 1994.

D. W. JORDAN & P. SMITH *Nonlinear ordinary differential equations*, Clarendon Press, Oxford, 1977.

H. P. KALMUS, *The inverted pendulum*, Amer. J. Phys. **38** (1970), 874–878.

P. L. KAPITSA, *Dynamic stability of a pendulum with a vibrating point of suspension*, Zh. Ehksp. Teor. Fiz. **21** (1951), 588–598 (Russian), translated version in *Collected papers by P. L. Kapitsa*, edited by D. ter Haar, Pergamon, Vol. 2, 714–726, London, 1965.

B. P. Koch, R. W. Leven, B. Pompe & C. Wilke, *Experimental evidence for chaotic behaviour of a parametrically forced pendulum*, Phys. Lett. A **96** (1983), 219–224.
B. P. Koch & R. W. Leven, *Subharmonic and Homoclinic bifurcations in a parametrically forced pendulum*, Phys. D **16** (1985) 1–13.
L. D. Landau & E. M. Lifshitz, *Mechanics*, 3rd Edn, Pergamon Press, Oxford, 1976.
T. Leiber & H. Risken, *Stability of parametrically exited dissipative systems*, Phys. Lett. A **129** (1988), 214–218.
R. W. Leven & B. P. Koch, *Chaotic behaviour of a parametrically excited damped pendulum*, Phys. Lett. A **86** (1981), 71–74.
R. W. Leven, B. Pompe, C. Wilke & B. P. Koch, *Experiments on periodic and chaotic motions of a parametrically forced pendulum*, Phys. D **16** (1985), 371–384.
M. M. Michaelis, *Stroboscopic study of the inverted pendulum*, Am. J. Phys **53** (1985), 1079–1083.
M. B. Monagan, K. O. Geddes, G. Labahn & S. Vorkoetter, *Maple V programming guide*, Springer, 1996.
M. Myers, R. Wicklin & P.Worfolk, *Dstool, A Dynamical System Toolkit with an Interactive Graphical Interface*, Center For Applied Mathematics, Cornell University (1991).
D. J. Ness, *Small oscillations of a stabilized, inverted pendulum*, Amer. J. Phys. **35** (1967), 964–967.
I. Percival & D. Richards, *Introduction to dynamics*, Cambridge University Press, Cambridge, 1982.
A. B. Pippard, *The inverted pendulum*, European J. Phys. **8** (1987), 203–206.
H. Poincaré, *Les Méthodes Nouvelles de la Méchanigue Céleste*, Vol. III, Gauthiers-Villars, Paris, 1899.
H. J. T. Smith & J. A. Blackburn, *Chaos in a parametrically damped pendulum*, Phys. Rev. A **40** (1989), 4708–4715.
H. J. T. Smith & J. A. Blackburn, *Experimental study of an inverted pendulum*, Amer. J. Phys. **60** (1992), 909–911.
A. Stephenson, *On a new type of dynamical stability*, Mem. Proc. Manch. Lit. Phil. Soc. **52** (1908), 1–10.